

# Growth and Electrical Studies of SbSeI

Archana Singh<sup>1</sup>, Harish K. Dubey<sup>2</sup>, D. E. Kshirsagar<sup>2</sup>, Vijay S Jadhav<sup>2</sup>

<sup>1</sup>Department of Chemistry, B. K. Birla College (Empowered Autonomous), Kalyan, India

<sup>2</sup>Department of Physics, B. K. Birla College (Empowered Autonomous), Kalyan, M.S., India]

**Abstract:** Needle-shaped shiny polycrystalline SbSeI was grown by Solid State Thermal Reaction of constituent elements taken in stoichiometric ratio in an evacuated quartz tube at 585 oC for 3.5 hours. The obtained compound was characterized by SEM, EDAX, and XRD techniques. The resistance vs. temperature curve exhibits the semiconducting nature of the compound with a resistivity of  $3.5 \times 10^7 \Omega\text{-cm}$ , an activation energy of 1.93 eV, and a dielectric constant of 10434. The photoconductive trait of the compound was studied in the visible region

**Index Terms:** SbSeI, Solid State Thermal Reaction, SEM, EDAX, XRD, resistivity, activation energy.

## I. INTRODUCTION

Chemical compounds consisting of at least one chalcogen anion and at least one more electropositive element are popularly known as Chalcogenides and are based on group 15-16-17 elements. AV BVI C VII (Where A= Sb, Bi; B= S, Se, Te and C= I, Cl, Br) compounds have been synthesized by many techniques. It is revealed from the literature that considerable attention has been paid to the ternary Chalcogenides possessing many interesting and useful properties like electronic, thermoelectric [1], Ferro electricity [2], and photoconductivity [3, 4]. These compounds are found useful in optoelectronic [4, 5, 6] devices, thermoelectric [5] piezoelectric devices [8], etc. Attempts have also been made to synthesize by various techniques and study the electrical properties [8, 9] of these materials. SbSI is one of the most intensively studied compounds, whereas the other compounds of this family have been less studied. Although the other Chalcogenides have been synthesized by many techniques [3], a simple and economical technique has been reported in this paper which was earlier used to synthesize SbSI of this family [8]. It is evident from the literature that the use of the elements Sb, S and I was avoided with a view that Sb, S and I unite exothermally generating a huge vapor pressure leading to the explosion but the

synthesis of SbSI by Chemical Vapor Deposition (CVD) technique using Sb, S and I as the starting material with a simple chemical equation:  $\text{Sb} + \text{S} + \text{I} = \text{SbSI}$  was reported [9, 10] and the synthesis of SbTeI was also reported by Dubey et al. with similar chemical reaction. Synthesis of SbSeI with Solid State Thermal reaction has been reported in this paper for the first time. The study of some interesting optoelectrical properties of SbSeI has been reported in this paper.

## II. EXPERIMENTAL

**A. Synthesis of SbSeI by Solid State Thermal Reaction:** SbSeI was synthesized by taking the stoichiometric ratio of Sb (1.5 gm), Se (0.973 gm) and I (1.563 gm) in a quartz tube of 16 cm length and 1.0 cm diameter. The tube was evacuated up to  $10^{-3}$  bar and sealed under vacuum. The tube was heated in a programmable muffle furnace at 585 OC for 3.5 hours (Fig. 1). The temperature of the furnace increased @45oC / min. It attains 585 oC after 16 min as seen from the temperature profile of the furnace. After the end of thermal treatment, the furnace was allowed to cool down slowly to room temperature. Crystals were seen grown in a bunch of grey shiny crystals (Fig 4). Some single crystals were seen on the inner walls of the tube (Fig. 1). The reaction involved in the process is  $\text{Sb} + \text{Se} + \text{I} = \text{SbSeI}$ .

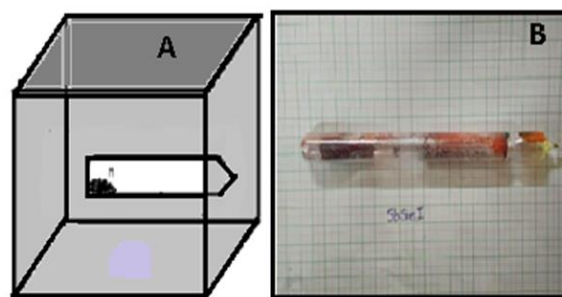


Figure 1. (A) Experimental Setup (B) Sealed evacuated ampule

**B. Characterization:**

Bunches of polycrystalline needle-shaped SbSeI crystals were cleaned with CS<sub>2</sub> and CCl<sub>4</sub>. The morphology was studied using SEM images of SbSeI using JEOL-6360 (LA) EDAX cum SEM. A probe current of 1 nA was set in the energy range of 0-20 KV for the scanning of the samples. The XRD pattern was recorded by a Phillips PW 3710 X-ray diffractometer using CuK $\alpha$  radiation. The scanning angle ( $\theta$ ) was set between 10 $^{\circ}$  to 80 $^{\circ}$

**C. Electrical Studies:**

Needle-shaped SbSeI crystal was powdered, and a pellet was made. The resistivity and activation energy of the material was calculated by finding the resistance of the sample in the temperature range of 30  $^{\circ}$ C to 100  $^{\circ}$ C. To obtain resistance of the pallet at different temperatures using a Two probe setup developed indigenously. To maintain an inert atmosphere Ar gas was passed continuously through the chamber containing the sample. To find the dielectric constant, the SbSeI pallet was sandwiched between two parallel plates, and its capacitance was measured at room temperature (30  $^{\circ}$ C). A plab L-C-R meter was used to find the capacitance at 1 KHz.

**D. Calculation of activation energy:**

Knowing the dimensions of the pallet under consideration i.e. its Surface area (A) and length (L), the resistivity ( $\rho$ ) of the sample is determined with the simple equation:

$$R = \rho * (L/A) \quad \dots\dots(1)$$

$$\text{and conductivity } (\sigma) = L/ \rho \quad \dots\dots(2)$$

As the temperature dependence of electrical conductivity ( $\sigma$ ) of semiconductors follows the Arrhenius law, the activation energy (E<sub>a</sub>) [11, 12] of semiconductors can be calculated by studying its conductivity ( $\sigma$ ) with respect to temperature (T). Equation 3 establishes a relation among these three quantities (Arrhenius law) as;

$$\sigma = \sigma_0 \exp (-E_a/kT) \quad \dots\dots(3)$$

where  $\sigma_0$  is the material's constant and K is the Boltzmann constant.

$$\text{Therefore, } \ln(\sigma) = \ln(\sigma_0) - (E_a/K) \dots\dots(4)$$

Thus if we plot a graph of  $\ln(\sigma)$  vs (1/T), the slope will be equal to E<sub>a</sub>/K.

i.e. (E<sub>a</sub>/K) = slope.

Therefore, E<sub>a</sub>= Slope x (8.6 X 10<sup>-5</sup>) eV

where, K = 8.6 X 10<sup>-5</sup> eV / $^{\circ}$ K.

Thus, when Ln ( $\sigma$ ) is plotted against inverse of temperature (1/T), normally one gets two straight lines – one at higher temperature and other at lower temperature. As a result of these two linear graphs, one exponential graph appears (Fig. 3). From this graph two linear graphs can be extracted as shown by dotted line in fig. 3. The slope of straight line is equal to (E<sub>a</sub>/K) where, E<sub>a</sub> is the activation energy. Activation energy calculated from higher temperature region represents the energy needed to excite the electrons for conductivity. If the material does not possess any impurities, this activation energy can be equivalent to half the band gap of the material [12]. Activation energy calculated from lower temperature region is equivalent to energy needed for making the excited electron to migrate in the material. This energy is normally very low. Negative sign in the equation is an indicator of negative slope of the graph. Fig. 6.3 gives a typical nature of  $\ln(\sigma)$  vs. (1/T) plot of a semiconductor.

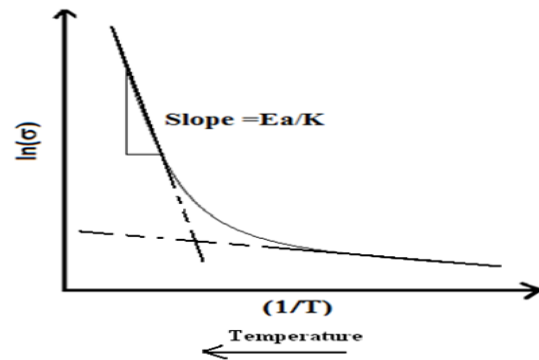


Figure 2: A typical  $\ln(\sigma)$  vs (1/T) plot for a semiconductor material.

**III. RESULTS AND DISCUSSION**

**A. Characterization:** The Powder XRD pattern SbSeI (Fig. 3) shows well defined, sharp peaks indicating high purity and well crystallized structure. All the diffraction peaks can be indexed to be a pure orthorhombic phase for SbSeI as indicated by the cell constants a=8.424 Å, b =10.628 Å, c =4.446 Å. The identification was done using the PCW computer program. In each XRD pattern, the reflections can be indexed to those of the corresponding pure phases. The lattice parameters are very close to the reported data [13]. The intensities and positions of the peaks are in good agreement with literature values for SbSeI [10].

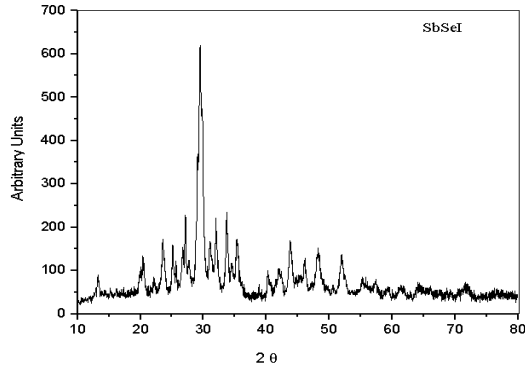


Figure 3. X-ray diffraction plot of SbSeI

Stoichiometric composition of SbSeI was calculated from the EDAX attached to the SEM unit. Composition of a prepared SbSeI shows Sb=36.47 %, Se=35.21% and I=28.32% in the ternary compound. So, it indicates within the experimental error a stoichiometric SbSeI. It is predominant from the SEM images (Fig. 5) that the compound synthesizes in shiny needle polycrystalline form. It is evident and supported by the sample photograph of a bunch of polycrystalline SbSeI with needles sizes as long as 0.8 cm (Fig. 4),

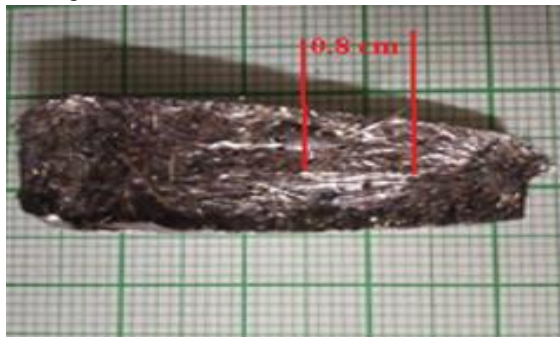


Figure 4: Bunch of SbSeI crystal synthesized by Solid State Thermal Reaction

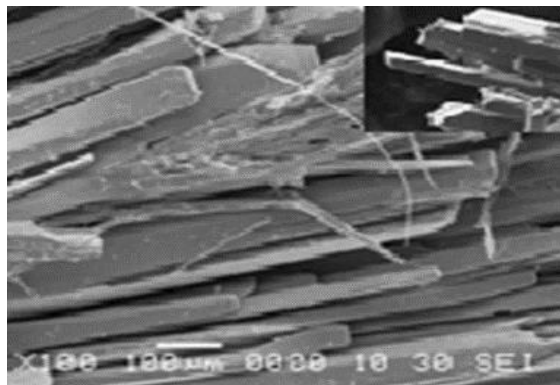


Figure 5. Scanning Electron Microscope image of SbSeI polycrystals

B. Electrical studies of SbSeI: A constant current (I) was passed through the sample and the voltage (V) developed across the pallet of the sample was noted down with an increase in temperature. The resistance (R) calculated from the values of I and V was found to be decreasing (Fig. 6) with the increase in temperature (30 to 100 oC) indicating the semiconducting nature of the sample as reported by Wibowo et. al [4]. The setup was also used to find the R Vs T study in the high temperatures range too. The resistivity of the sample was calculated to be  $3.5 \times 10^7 \Omega\text{-cm}$ . The high resistivity also supports the higher value of activation energy which was calculated to be 1.93 eV by plotting a graph of  $\ln(\sigma)$  vs  $(1/T)$ . The dielectric constant was found to 10434 at 30 oC measured at 1 KHz.

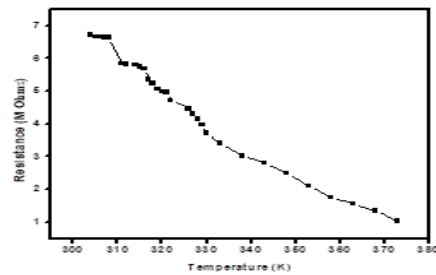


Figure 6: Variation of Resistance with Temperature of SbSeI

#### IV. CONCLUSION

Gray shiny needle shaped polycrystalline ternary Chalcogenide SbSeI was synthesized by Solid State Thermal Reaction technique at 5850C for 3.5 hours. The XRD, SEM and EDAX characterization confirms the formation of the Compound. The lattice parameters and the SEM images confirm the compound to be orthorhombic. Resistance Vs Temperature curve indicate the compound to be semiconducting in nature. The compound exhibits high resistivity at room temperature in the order of  $10^7 \Omega\text{-cm}$  whereas the dielectric constant was found to 10434 at 30 oC. The activation energy was calculated to be 1.93 eV.

#### V. REFERENCES

##### A. Figures and Tables

Because the final formatting of your paper is limited in scale, you need to position figures and tables at the top and bottom of each column. Large figures and tables may span both columns. Place figure captions

below the figures; place table titles above the tables. If your figure has two parts, include the labels —(a) and —(b) as part of the artwork. Please verify that the figures and tables you mention in the text actually exist. Do not put borders around the outside of your figures. Use the abbreviation —Fig. even at the beginning of a sentence. Do not abbreviate —Table. Tables are numbered with Roman numerals. Include a note with your final paper indicating that you request color printing. Do not use color unless it is necessary for the proper interpretation of your figures. There is an additional charge for color printing. Figure axis labels are often a source of confusion. Use words rather than symbols. As an example, write the quantity—Magnetization, or —Magnetization M, not just —M. Put units in parentheses. Do not label axes only with units. As in Fig. 1, for example, write —Magnetization (A/m) or Magnetization ( $A \cdot m^{-1}$ ), not just —A/m. Do not label axes with a ratio of quantities and units. For example, write —Temperature (K), not —Temperature/K. Multipliers can be especially confusing. Write—Magnetization (kA/m) or —Magnetization ( $10^3$  A/m). Do not write —Magnetization (A/m) X 1000 because the reader would not know whether the top axis label in Fig. 1 meant 16000 A/m or 0.016 A/m. Figure labels should be legible, approximately 8 to 12 point type.

#### REFERENCE

1. Wilayat Khan, Sajjad Hussain, Jan Minar and Sikander Azam. Journal of electronic materials, Volume 47, Issue 2, (2017) 1131–1139.
2. E. Fatuzzo, G. Harbete, W. J. Merz, R. NMerz, R. Nitsche, H. Roetschi, W. Ruppel. Physics Review. Vol 127 No. 6, (1962) 2036.
3. R. Nitsche and W.J. Merz, Journal of Physical Chemistry Solids, Vol. 13. (1960) 154-155.
4. Arief C. Wibowo, Christos D. Malliakas, Zhifu Liu, John. A. Peters, Maria Sebastian, Duck Young Chung, Bruce W. Wessels, Mercouri G. Kanatzidis, *norg. Chem.* 2013, 52, 12, 7045-7050.
5. Bo Peng, Ke Xu, Hao Zhang, Zeyu Ning, Hezhu Shao, Gang Ni, Jing Li, Yongyuan Zhu, Heyuan Zhu, Costas M. Soukoulis, Wiley Online library, 2018.
6. Soonie Jeon, Gijun Cho, Wha-Tek Kim, Sook-II Kwun, Solid State Communication, Vol. 8, Issue 11 (1988) 1043-1046.

7. Berlincourt D., Hans Jaffe, Merz W. J. and Nitsche R. (1964), Applied Physics letters Vol.4 Issue 3 (1964) 61.
8. Harish K. Dubey, L. P. Deshmukh, D. E. Khirsagar, Madhuri Sharon and Maheshwar Sharon. Advances in Physical Chemistry, Vol. 2014 (2013) 1-6.
9. Harish K. Dubey, L.P. Deshmukh, D. E. Kshirsagar, Vijay S. Jadhav, Madhuri Sharon and Maheshwar Sharon, J. Nepal Chem. Soc. 30 (2011), 11.
10. M. Nowak, B. Kauch, P. Szperlich, M. Jesionek, M. Kepinska, L. Bober, J. Szala, G. Moskal, T. Rzychon, D. Stroz. Ultrasonics Sonochemistry, 16 (2009) 546-551.
11. Patidar D., Rathore K. S., Saxena N. S., Sharma Kananbala and Sharma T. P., Chalcogenide Letters Vol. 5(2) (2008):21
12. Nkum R. K., Adimado A. A. and Totoe H.), Material Science and Engineering, B55 (1998) :102
13. G. P. Voutsas and P. J. Rentzeperis, Zeitschrift für Kristallographie- Crystalline Materials, Vol. 161 (1982): Issue 1-2.